

Alternating-gradient focusing and deceleration of large molecules

Kirstin Wohlfart, Fabian Grätz, Frank Filsinger, Henrik Haak, Gerard Meijer, and Jochen Küpper*

Fritz-Haber-Institut der Max-Planck-Gesellschaft, Faradayweg 4-6, 14195 Berlin, Germany

(Received 26 November 2007; published 24 March 2008)

We have focused and decelerated benzonitrile (C_7H_5N) molecules from a molecular beam, using an array of time-varying inhomogeneous electric fields in alternating-gradient configuration. Benzonitrile is prototypical for large asymmetric top molecules that exhibit rich rotational structure and a high density of states. At the rotational temperature of 3.5 K in the pulsed molecular beam, many rotational states are populated. Benzonitrile molecules in their absolute ground state are decelerated from 320 to 289 m/s, and similar changes in velocity are obtained for excited rotational states. All measurements agree well with the outcome of trajectory calculations. These experiments demonstrate that such large polyatomic molecules are amenable to the powerful method of Stark deceleration.

DOI: [10.1103/PhysRevA.77.031404](https://doi.org/10.1103/PhysRevA.77.031404)

PACS number(s): 37.10.Mn, 33.15.-e, 37.20.+j, 87.15.-v

The production of cold molecular samples offers fascinating prospects for fundamental physics studies [1,2] and ultracold chemistry [3]. One of the many techniques developed for the production of cold molecules [4] relies on the deceleration of polar molecules from a molecular beam using an array of time-varying inhomogeneous electric fields [5]. In recent years, tremendous advances have been made in the Stark deceleration and trapping of small, polar molecules in low-field-seeking (lfs) states [6–9]. For large molecules with a dense manifold of rotational states, however, all states are high-field seeking (hfs) at the relevant electric field strengths. To confine such molecules a maximum of the electric field on the molecular beam axis would be needed, which cannot be created using static electric fields. Therefore, dynamic focusing—also referred to as alternating-gradient (AG) focusing—has to be used [10]. In order to decelerate the molecules, the longitudinal electric field gradients at the exit of the AG lens are exploited. So far, only a few proof-of-principle experiments on the AG focusing and deceleration of diatomic molecules (metastable CO and YbF) in hfs states have been performed [11–13]. Complementary, slow beams of thermally stable large molecules can directly emerge from an oven [14]. However, these samples are internally hot (~ 600 K) and, therefore, the population is distributed over a large number of quantum states and different conformers.

It is important to experimentally demonstrate that AG focusing and deceleration also work for large molecules, in order to produce cold, slow samples thereof. This would vastly extend the range of species whose motion and orientation can be precisely controlled. In particular, this would enable novel studies on the “molecular building blocks of life.” During recent decades, structural and dynamical properties of these biomolecules have been unraveled via detailed spectroscopic studies on isolated systems in the gas phase [15–17]. In these studies, the advances in the preparation of beams of internally cold biomolecules have been instrumental. The control over the velocity of the molecules provided by the AG decelerator would enable increased observation

times, and thereby, in principle, a higher spectral resolution. This would have a possible application in the search for parity violation in chiral molecules [1]. Furthermore, the rotational state selection intrinsic to the AG focusing and deceleration process would result in less congested spectra. In a molecular beam, biomolecules occur in multiple conformational structures [18,19]. For tryptophan, for example, six conformers have been observed [19,20] with their calculated dipole moments ranging from 1 to 7 D. The state selection in the AG decelerator would naturally provide packets of selected conformers. These state- and conformer-selected packets of molecules can be strongly aligned or oriented. They would, for instance, be highly beneficial for electron or x-ray-diffraction imaging studies [21,22], where disentangling the overlaying contributions from different species would be an onerous task. The tunable velocity and the narrow velocity distribution of the AG decelerated beams would also be of great advantage for matter wave interferometry experiments [23].

Here we demonstrate the AG focusing and deceleration of benzonitrile (C_7H_5N), a prototypical large molecule. Benzonitrile is an asymmetric rotor and has a dense rotational level structure. The Stark effect is due to the coupling of closely spaced rotational states by an electric field [24]. Experiments are performed with benzonitrile in various rotational states, including its absolute ground state $J_{K_a K_c} = 0_{00}$. This is the only state that is stable against collisions at sufficiently low temperatures. Excited rotational states have the added complication of real and avoided crossings of levels as a function of the electric field strength. It is not *a priori* clear whether one can focus and decelerate molecules in states within such a dense Stark manifold [25,26]. However, we successfully demonstrate this for the 4_{04} state. All measurements agree well with the outcome of trajectory calculations.

The experimental setup is shown in Fig. 1(a). Benzonitrile is co-expanded in 0.7 bar of xenon at a temperature of 300 K through a pulsed nozzle with a 0.8 mm orifice and an opening time of about 150 μ s. The experiments are performed at a repetition rate of 40 Hz. The molecular beam has a velocity of approximately 320 m/s and a full width at half maximum (FWHM) velocity spread of about 10%. The molecules pass through a 1.5-mm-diam skimmer mounted directly on a gate

*Author to whom correspondence should be addressed: jochen@fhi-berlin.mpg.de

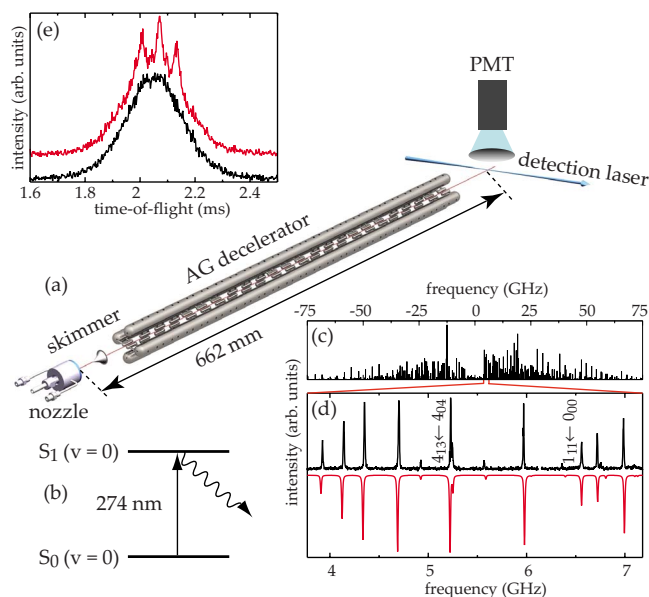


FIG. 1. (Color online) (a) Schematic view of the experimental setup. (b) LIF detection scheme. (c) Simulated rotationally resolved electronic excitation spectrum of benzonitrile at the rotational temperature of 3.5 K. The frequencies are given relative to the origin at $36\,512.74\text{ cm}^{-1}$. (d) Expanded view of the experimental (upper black trace) and simulated (lower red trace) spectrum. (e) Time-of-flight profiles of benzonitrile in its ground state. The lower (black) trace depicts the free-flight signal, and the upper (red) trace, which is offset for clarity, depicts the signal for optimum focusing conditions.

valve [27], and then enter the AG decelerator. The decelerator starts 37 mm behind the tip of the skimmer and consists of 27 AG lenses arranged along the molecular beam axis. Each lens consists of a pair of 13-mm-long electrodes with a diameter of 6 mm and spherical end caps. The two parallel electrodes within each lens have an opening of 2 mm between them. Successive lenses are placed at center-to-center distances of 20 mm and are rotated relative to each other by 90° after every third lens, adding up to a total length of the decelerator of 533 mm. The positioning of the electrodes is accurate to about 0.1 mm. For all pairs of electrodes, voltages are switched between $\pm 15\text{ kV}$ and ground, resulting in a maximum electric field of 143 kV/cm. An additional bias voltage of up to $\pm 0.3\text{ kV}$ is applied for the suppression of unwanted transitions between levels at zero field.

Benzonitrile molecules are detected 662 mm behind the nozzle by laser-induced fluorescence (LIF) at 274 nm using time-resolved photon counting. A frequency-doubled and frequency-stabilized, narrow-linewidth, continuous ring dye laser is used for state-specific detection. A part of the experimental $S_1 \leftarrow S_0$ excitation spectrum is shown in Fig. 1(d), where the individual rovibronic transitions are clearly resolved. The spectrum is simulated [28] using the known molecular constants [29,30]. Full agreement with the measured spectrum is achieved using a rotational temperature of 3.5 K, the known natural linewidth (FWHM) of 8 MHz [29], and a Gaussian contribution of 7.5 MHz which accounts for Doppler broadening and the laser linewidth. To record the time-

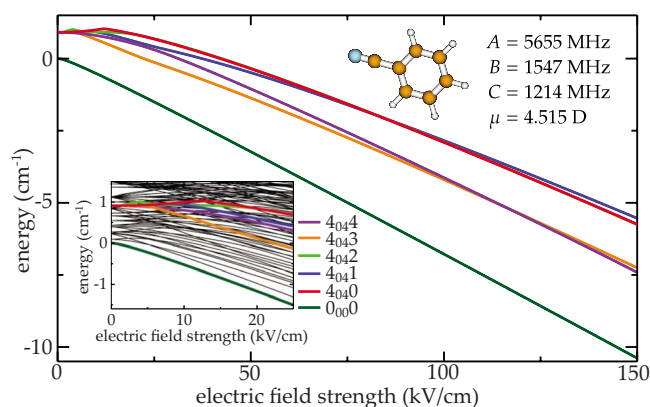


FIG. 2. (Color online) Energies of all M levels of the examined rotational states $J_{K_a K_c} M = 0_{00}0$ and $4_{04}M$ ($M = 0, \dots, 4$) of benzonitrile as a function of the electric field strength. The structure, the rotational constants, and the dipole moment of benzonitrile are given in the upper right corner. The inset illustrates the energies of the lowest levels for small electric field strengths.

of-flight (TOF) distribution in a given state, the laser is set to the desired transition frequency. TOF profiles for the 0_{00} state are shown in Fig. 1(e), both for free flight, i.e., when no voltages are applied to the decelerator, and for optimum focusing conditions. When the high voltages are on, a structured TOF distribution is observed containing a background that resembles the free-flight distribution. The peak intensity of the focused molecules is enhanced by 30% with respect to that of the molecules in free flight. In the remainder, we show and discuss the difference-TOF profiles, obtained by taking the difference of the measurements with and without electric fields.

The rotational constants of benzonitrile and its dipole moment are precisely known [30]. Therefore, the Stark curves and the trajectories of benzonitrile in an AG decelerator can be accurately calculated. The energies of the relevant levels are shown in Fig. 2 as a function of the electric field strength. The rotational ground state 0_{00} has only a single M level, whereas the 4_{04} state splits into five M levels. For all excited rotational states real and avoided level crossings occur at low electric field strengths, as is shown for the 4_{04} state.

To describe the sequence of times at which the high voltages are switched, we use the concept of a synchronous molecule, which is by definition always at the same position within an AG lens when the high voltages are switched. The time interval during which the high voltages are applied to an AG lens, in combination with the velocity of the synchronous molecule, determine the focusing length f . The amount of kinetic energy that is removed per AG lens depends on the position of the synchronous molecule on the molecular beam axis at the time when the high voltages are switched off. This position, relative to the center of the AG lens, is denoted by d .

Figure 3 illustrates the focusing behavior of the 0_{00} and 4_{04} states of benzonitrile for a constant velocity of the synchronous molecule of 320 m/s. The high voltages are switched on symmetrically around the centers of the AG lenses. Therefore, the molecular packet is focused in both

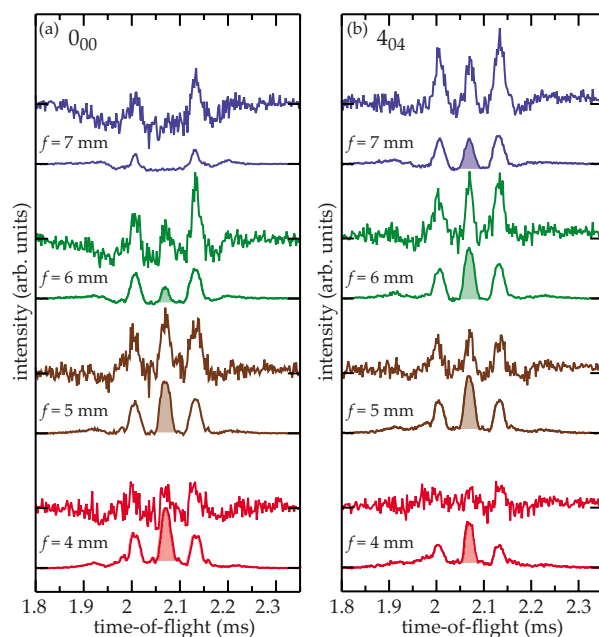


FIG. 3. (Color online) Sequence of difference-TOF profiles for the (a) 0_{00} and (b) 4_{04} states of benzonitrile obtained using different focusing lengths f for a constant velocity of 320 m/s. The upper traces show the difference between the experimental TOF profiles with and without high voltages applied. The lower traces show the corresponding simulations, where the packets containing the synchronous molecule have been shaded.

transverse directions as well as in the longitudinal direction (bunching), but no change of the synchronous velocity occurs. In the experiments three packets of focused molecules are observed. The central peaks of the TOF distributions occur 2.07 ms after the molecules exit the nozzle. These packets contain the synchronous molecule. Hereafter, they are referred to as the “synchronous packets,” and they are shaded in the simulated TOF distributions. The peaks at earlier and later arrival times correspond to molecular packets leading and trailing the synchronous packet by one AG lens (or 20 mm), respectively. These packets are also focused in all three dimensions. However, due to the lens pattern in our setup, they experience only 2/3 of the lenses at high voltage. This results in a reduced overall focusing for these packets.

For the focusing of the 0_{00} state it is seen that the synchronous packet is most intense for a focusing length of $f=5$ mm. Under these conditions approximately 10^5 molecules per quantum state per pulse are confined in the phase-stable central peak, corresponding to a density of 10^7 cm $^{-3}$. For smaller focusing lengths a shallower time-averaged confinement potential is created, and fewer molecules are guided through the decelerator. For larger focusing lengths the molecular packet is overfocused, also resulting in a decreased transmission. For $f=7$ mm the overfocusing is so severe that the synchronous packet completely disappears. As expected, the nonsynchronous packets benefit from the increased focusing lengths. Figure 3(b) shows the focusing behavior for the 4_{04} state. The observed focusing effects are similar to those for the 0_{00} state. Due to the smaller Stark shifts of the five M levels, a larger optimum focusing length

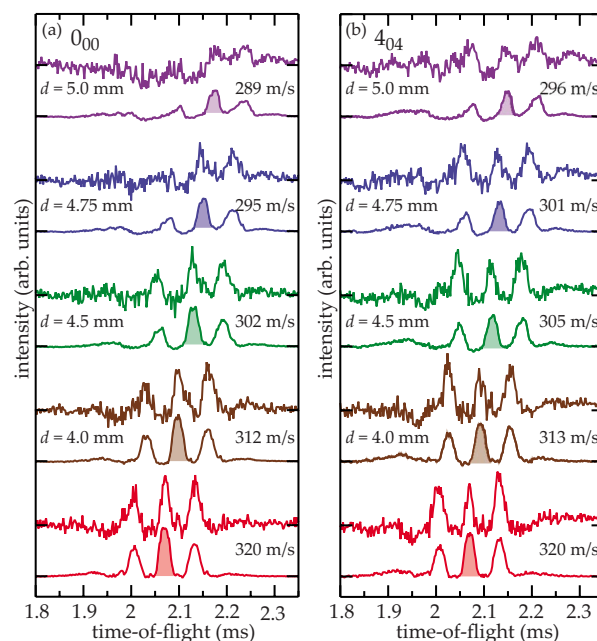


FIG. 4. (Color online) Sequence of difference-TOF profiles for the deceleration of the (a) 0_{00} and (b) 4_{04} states of benzonitrile from an initial velocity of 320 m/s to the indicated final velocities. The positions d that have been used to reach these final velocities are specified (see the text for details). The upper traces show the difference between the experimental TOF profiles with and without high voltages applied. The lower traces show the corresponding simulations, where the packets containing the synchronous molecule have been shaded.

of $f=6$ mm is found for the synchronous packet. Moreover, each of these M levels has a distinct Stark curve and, therefore, a distinct focusing behavior. The measured TOFs are the sums of these five individual contributions, resulting in a considerably weaker dependence of the overall transmission on the exact focusing length. The simulated TOF distributions obtained from trajectory simulations match the experimental results very well. It should be noted that all simulated profiles are scaled down by a factor of 17. Extensive simulations indicate that this can be attributed to mechanical misalignment of the electrodes on the order of 0.1 mm. No additional losses for the 4_{04} state compared to the 0_{00} state are observed, demonstrating that transitions between different states at avoided crossings are not as severe as might have been anticipated [25,26].

Figure 4 presents the results for the deceleration of benzonitrile in its 0_{00} and 4_{04} states. The bottommost (red) traces show focusing experiments for a constant velocity of the synchronous molecule of 320 m/s using the optimum focusing lengths. All other traces show experiments in which the synchronous packet is decelerated from 320 m/s to successively lower velocities, resulting in later arrival times at the detector. Using $d=5$ mm, the packet is decelerated to 289 m/s, corresponding to a reduction of the kinetic energy by 18%. The observed intensities of the nonsynchronous packets decrease faster upon increasing d . Because the molecules in these packets miss every third deceleration stage, their trajectories are not stable and they are only observed

due to the finite length of the decelerator. When deceleration to lower velocities is performed by increasing d the signal intensity decreases due to the reduction in phase-space acceptance. However, one could also decelerate to lower velocities by increasing the number of AG lenses for a given value of d . In this case, in principle, no decrease in the intensity of the synchronous packet is expected due to the phase stability of the deceleration process [13]. The deceleration behavior of the 4_{04} state, shown in Fig. 4(b), is similar to that of the ground state. However, it is important to realize that the optimum deceleration time sequences differ for the individual M levels. Using time sequences calculated for the $M=0$ level, the synchronous packet is decelerated to successively lower final velocities, down to 296 m/s. Apart from slightly different final velocities and intensities, analogous results are obtained for time sequences calculated for other M levels. For a considerably longer decelerator and a given time sequence, the M levels could, in principle, be separated based on their different Stark shifts. For all deceleration measurements, the relative intensities and the arrival times of the molecular packets at the detector are nicely reproduced by the trajectory simulations.

In conclusion, we have demonstrated that alternating-gradient focusing and deceleration can be performed for large asymmetric top molecules. We have examined the focusing properties for benzonitrile in several low-lying rotational states. Benzonitrile has been decelerated both in its absolute ground state and in excited rotational states. Focusing and deceleration have also been demonstrated for the 1_{01} and 6_{06} states (not shown). If desired, different rotational states can be decelerated simultaneously, albeit with different acceptances. It should be realized, that already in the current

experiment a significant amount of state selection is achieved. Whereas the different low-energy rotational states investigated in this work are focused and decelerated with similar acceptances, higher rotational states often have negligible Stark shifts and are practically not accepted by the decelerator.

Currently we are extending the decelerator to 81 deceleration stages, using refined mechanical alignment procedures and an improved lens pattern, where we rotate the focusing direction every two stages. With this setup we expect to be able to decelerate benzonitrile molecules from 320 to 150 m/s, removing about 80% of the kinetic energy, with intensities about an order of magnitude smaller than the ones reported here. For the deceleration to even lower velocities and eventually loading the molecules into a trap, hyperbolic electrode geometries will be used [13]. Three-dimensional confinement is possible, for instance, in ac electric traps, in which the very same principles of dynamic focusing as in the AG decelerator are employed [31]. This will enable us to select and decelerate conformers of large molecules, such as the amino acid tryptophan or small model peptides, to low velocities, and eventually trap them. This would allow one to precisely study the intrinsic properties of these species, for example, dynamical processes on time scales ranging from femtoseconds to fractions of a second, i.e., interconversion between conformational structures.

This work would not have been possible without the technical support at the FHI. Helpful discussions with Hendrick L. Bethlem as well as financial support from the Deutsche Forschungsgemeinschaft within the priority program 1116 “Interactions in Ultracold Gases” are gratefully acknowledged.

-
- [1] C. Daussy *et al.*, Phys. Rev. Lett. **83**, 1554 (1999).
 [2] J. J. Hudson, B. E. Sauer, M. R. Tarbutt, and E. A. Hinds, Phys. Rev. Lett. **89**, 023003 (2002).
 [3] R. V. Krems, Int. Rev. Phys. Chem. **24**, 99 (2005).
 [4] Special issue of Eur. Phys. J. D **31** (2), 149 (2004).
 [5] H. L. Bethlem, G. Berden, and G. Meijer, Phys. Rev. Lett. **83**, 1558 (1999).
 [6] H. L. Bethlem *et al.*, Nature (London) **406**, 491 (2000).
 [7] S. Y. T. van de Meerakker, P. H. M. Smeets, N. Vanhaecke, R. T. Jongma, and G. Meijer, Phys. Rev. Lett. **94**, 023004 (2005).
 [8] C. E. Heiner, D. Carty, G. Meijer, and H. L. Bethlem, Nat. Phys. **3**, 115 (2007).
 [9] B. C. Sawyer *et al.*, Phys. Rev. Lett. **98**, 253002 (2007).
 [10] D. Auerbach, E. E. A. Bromberg, and L. Wharton, J. Chem. Phys. **45**, 2160 (1966).
 [11] H. L. Bethlem, A. J. A. van Roij, R. T. Jongma, and G. Meijer, Phys. Rev. Lett. **88**, 133003 (2002).
 [12] M. R. Tarbutt *et al.*, Phys. Rev. Lett. **92**, 173002 (2004).
 [13] H. L. Bethlem *et al.*, J. Phys. B **39**, R263 (2006).
 [14] S. Deachapunya *et al.*, Eur. Phys. J. D **46**, 307 (2008).
 [15] Special issue of Eur. Phys. J. D **20** (3), 309 (2002).
 [16] Special issue of Phys. Chem. Chem. Phys. **6** (10), 2543 (2004).
 [17] M. S. de Vries and P. Hobza, Annu. Rev. Phys. Chem. **58**, 585 (2007).
 [18] R. D. Suenram and F. J. Lovas, J. Am. Chem. Soc. **102**, 7180 (1980).
 [19] T. R. Rizzo, Y. D. Park, L. Peteanu, and D. H. Levy, J. Chem. Phys. **83**, 4819 (1985).
 [20] L. C. Snoek, R. T. Kroemer, M. R. Hockridge, and J. P. Simons, Phys. Chem. Chem. Phys. **3**, 1819 (2001).
 [21] K. Hedberg *et al.*, Science **254**, 410 (1991).
 [22] H. N. Chapman *et al.*, Nat. Phys. **2**, 839 (2006).
 [23] S. Gerlich *et al.*, Nat. Phys. **3**, 711 (2007).
 [24] W. Gordy and R. L. Cook, *Microwave Molecular Spectra*, 3rd ed. (Wiley, New York, 1984).
 [25] E. Vliegen, H. J. Wörner, T. P. Softley, and F. Merkt, Phys. Rev. Lett. **92**, 033005 (2004).
 [26] M. Abd El Rahim *et al.*, J. Phys. Chem. A **109**, 8507 (2005).
 [27] J. Küpper, H. Haak, K. Wohlfart, and G. Meijer, Rev. Sci. Instrum. **77**, 016106 (2006).
 [28] C. M. Western, Pgopher (University of Bristol, UK, 2007).
 [29] D. R. Borst, T. M. Korter, and D. W. Pratt, Chem. Phys. Lett. **350**, 485 (2001).
 [30] K. Wohlfart, M. Schnell, J.-U. Grabow, and J. Küpper, J. Mol. Spectrosc. **247**, 119 (2008).
 [31] J. van Veldhoven, H. L. Bethlem, and G. Meijer, Phys. Rev. Lett. **94**, 083001 (2005).